Energy Reports 7 (2021) 9023–9034

Contents lists available at ScienceDirect

Energy Reports

journal homepage: www.elsevier.com/locate/egyr

Research paper

Investigations of double layer phase change walls with expanded graphite on the temperature and energy consumption

Hanxue Yang [a], Guanhua Zhang [a,*], Binlin Dou [a], Xiaoyu Yan [b], Zhiqiang Liu [c], Wenchao Qi [d]

[a] School of Energy and Power Engineering, University of Shanghai for Science and Technology, Shanghai, 200093, China
[b] Environment and Sustainability Institute, University of Exeter, Penryn, Cornwall, TR10 9FE, UK
[c] China Aviation Technology Hangzhou Co., Ltd. Hangzhou, 310012, China
[d] Sinopec Nanjing Engineering Co., Ltd. Nanjing 211100, China

ARTICLE INFO

Article history:
Received 6 August 2021
Received in revised form 8 November 2021
Accepted 15 November 2021
Available online 6 December 2021

Keywords:
Phase change wall
Expanded graphite
Maintain temperature
Indoor thermal comfort
Building energy saving

ABSTRACT

In this paper, a composite structure double layer phase change walls with expanded graphite (EG) was investigated. By adding the EG, the time needed for the phase change process and the wall to work was both accelerated. The effect of composite phase change walls on the indoor thermal comfort and building energy consumption were investigated experimentally. The results show that the double layer phase change wall with the EG can suppress the temperature fluctuation. In addition, it simulated the cooling and heating loads with or without phase change walls based on the climatic conditions in Shanghai. The results show that the heating load in winter is reduced by more than 15%. The simulated values are consistent with the experimental values, and the temperature deviation at the same measuring point within the same period is small. The maximum temperature change between the experimental and simulated values is less than 1 °C. The double layer phase change wall with the EG can reduce the temperature fluctuation and improve the indoor thermal comfort.

1. Introduction

With the further study of renewable energy, it is found that energy storage system can solve the imbalance between energy supply and demand, improve and upgrade the energy structure better (Gil et al., 2010; Yun et al., 2020). Today, energy storage systems are increasingly being used to save energy in buildings, with the aim of reducing their dependence on fossil fuels for more efficient and reliable heating (Cellura et al., 2018; Wang et al., 2020).

At the beginning of the new century, researchers gradually applied phase change materials (PCMs) to building energy storage walls (Du et al., 2018). Its outstanding feature is that the wall can store the sensible and latent heat. When the temperature rises during the day, the PCM absorbs solar energy and begins to melt, preventing the heat being transferred to the room (Markarian and Fazelpour, 2019; Gholamibozanjani and Farid, 2020). When the temperature decreases at night, the PCM solidifies and releases the heat. This in turn reduces the indoor temperature fluctuations of the building (Saxena et al., 2020; Lin et al., 2018).

The PCM materials is manifested in three aspects (Ghadbeigi et al., 2018; Lu et al., 2020; Wang et al., 2019): phase change energy storage envelope, heating energy storage system and phase change air conditioning system. PCMs employed as a solution to reduce energy consumption and greenhouse gas emissions (Skaalum and Groulx, 2020; Zhang et al., 2018, 2020). Scholars have done intensive experiments and exploration on the whole process of building energy conservation (Zhang et al., 2018, 2020). The PCMs and traditional building materials are made into walls, roofs, floors, thereby these building structures have a certain ability to store the heat. Bao et al. (2020) utilized inorganic PCM $CaCl{\cdot}6H_2O$ to make building walls, and flake graphite was used to reduce the supercooling of the material. The simulation results indicated that the application in Hong Kong and Changsha were economically feasible with the payback periods of 18.3 years and 8.4 years respectively. Yang et al. (2019) developed a "PCM cool roof system" and to evaluate its performance by applying the specific system to the roof envelop. Research results showed that when used the PCM cool roof system, the roof surface temperature could be reduced in all seasons. The maximum temperature difference was 2.5 °C in winter and 5.7 °C in summer. Mankel et al. (2019) made ordinary mortar and porous recycled brick aggregate into spherical mortar and filled with liquid paraffin. The experimental results showed that the material reduced the internal temperature fluctuations, and the strength loss caused by the addition of PCM was almost negligible.

In order to investigate the thermal performance of the PCM wall and optimize the application of PCMs, Xie et al. (2018b)

* Corresponding author.
E-mail address: guanhuazhang@usst.edu.cn (G. Zhang).

https://doi.org/10.1016/j.egyr.2021.11.237

designed a set of thermal performance test equipment, and they conducted a case where the solar energy suddenly irradiated the PCM layer during the day and disappeared in the air-conditioned room at night. Liu et al. mixed (Liu et al., 2019a) paraffin/expanded graphite (EG) to form composite PCM, then added foam, stirred and poured into the mould to prepare a type of foamed cement insulation block. Due to its porous structure, foamed cement has lightweight and high thermal insulation capacity. The composite phase change energy storage material was combined with the building to prepare the energy storage wall for the solar house (Roman et al., 2016; Behi et al., 2018). Not only the wall has better thermal insulation performance, but it can also maintain a comfortable temperature in the room (Fu et al., 2017; Li et al., 2017; Chen et al., 2017; Liu et al., 2020). In order to achieve better results, other researchers built double layer wall and floor with PCM (Jin and Zhang, 2011; Zhu et al., 2016). Although they achieved certain temperature suppression effect (Zhu et al., 2019a,b), there were limited analysis on the energy consumption, and the thickness of the wall was generally thick.

Paraffin is a widely used organic PCM, which is non-toxic, non-corrosive and inexpensive, it has been well investigated (Maleki et al., 2019; Fredi et al., 2019; Chen et al., 2020). However, paraffin has poor thermal conductivity and slow melting speed. EG has excellent cold resistance, heat resistance, corrosion resistance, self-lubrication and other properties, but it also has the characters of softness, compression resilience, adsorption, ecological environment coordination, biocompatibility and radiation resistance, that natural graphite does not have (Qu et al., 2020; Xie et al., 2018a). Adding EG to the PCM can improve the thermal conductivity, and has little effect on the latent heat of the PCM (Ziasistani and Fazelpour, 2019).

EnergyPlus simulation software includes the Conducting Finite Difference (CondFD) algorithm, which was utilized to simulate the impact of building envelopes and HVAC on the indoor energy consumption. Numerous scholars have used EnergyPlus to investigate the effect of PCMs in building energy saving (Dutkowski and Fiuk, 2018; Liu et al., 2019b).

Based on the previous researches, this article breaks through the limitations of applying PCMs to single walls, it also uses a double layer PCM to achieve a thinner functional wall. In addition, the EG was applied on the PCM walls to enhance the heat conduction of PCM wall. In the winter, the internal phase change wall absorbs the heat and prevents the heat loss, and in the summer both internal and external phase change walls can achieve heat absorption and heat insulation. Therefore, a double layer PCM walls can be employed to regulate the indoor temperature in the summer and winter respectively. For the south wall and roof that mainly receive solar radiation, it applied 29 °C PCM on the external wall and 18 °C PCM on the internal wall. For floors with high indoor heat dissipation, 18 °C PCM was also applied. In addition, in order to verify the experiment, EnergyPlus software was utilized to simulate and analyse the energy-saving effect of the building models, meanwhile the internal temperature changes and energy consumption of air conditioning in Shanghai were compared. The effect of phase change walls on the indoor thermal comfort and building energy consumption were also investigated.

2. Simulation method

2.1. Description of simulated model

The size of the physical model is 30 cm × 30 cm × 30 cm, and the structure diagram is shown in Fig. 1(a). The model mainly employed double layer PCMs to receive the solar radiation on the top and south sides. The diagram of its composition is shown in Fig. 1(b) The wall structure comprises of a PCM layer 1, a heat insulation layer, a concrete layer, a heat insulation board layer and a PCM layer 2 in order from the outside to the inside. The thermophysical properties parameters of PCMs are presented in Table 2.

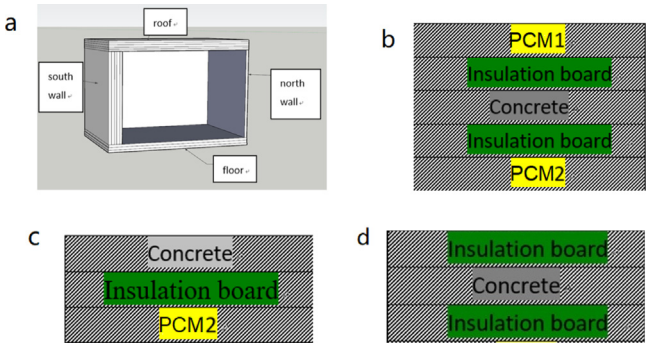

Fig. 1. (a) Physical model of experimental group, (b) Double layer phase change wall (roof and south wall), (c) Single layer shaped phase change wall (floor) and (d) The wall without PCMs (east, west and north wall).

Table 1
Thermophysical properties of materials.

	Insulation board	Concrete
Thermal conductivity/[W/(m K)]	0.31	0.02
Density/(kg/m^3)	1600	2500
Thickness/mm	10	10
Specific heat [J/(kg K)]	1160	90
Thermal diffusivity/($\times 10^{-7}$ m^2/s)	5.45	3.05

Table 2
Thermophysical properties of PCMs.

Sample	Phase-transition temperature (°C)	Latent heat of phase change (J/g)	Onset temperature (°C)	Endset temperature (°C)
PCM1	18.0	182.0	18.1	36.0
PCM2	29.0	178.0	29.1	48.0

The floor material, which is showing in Fig. 1(c), is a single layer of PCM. From the outside to the inside, the wall structure is a concrete layer, a heat insulation board layer and a PCM layer 2 in sequence. Since the east, west and north sides receive less solar radiation, no PCMs were applied in these three walls and these walls are only concrete layers, and Fig. 1(d) shows a schematic of these walls. Table 1 shows the wall thickness and the parameters of the materials used. The cubic models in the reference group and the experimental group is the same size, the wall, roof and ground are all constructed without PCM. The composition is like the structure in Fig. 1(d).

2.2. Governing equations

In EnergyPlus 9.0, the simulation of melting and solidification of PCM materials are mainly based on the one-dimensional finite difference equation of heat conduction (Chen et al., 2017; Liu et al., 2020).

$$C_p \rho \Delta X \frac{T_i^{j+1} - T_i^j}{\Delta t} = k_w \frac{(T_{i+1}^{j+1} - T_i^{j+1})}{\Delta X} + k_e \frac{(T_{i-1}^{j+1} - T_i^{j+1})}{\Delta X} \quad (1)$$

$$k_w = \frac{(k_{i+1}^{j+1} + k_i^{j+1})}{2} \quad (2)$$

$$k_e = \frac{(k_{i-1}^{j+1} + k_i^{j+1})}{2} \quad (3)$$

$$\Delta x = \sqrt{c\alpha\Delta t} = \sqrt{\frac{\alpha\Delta t}{Fo}} \tag{4}$$

$$h = h(t) \tag{5}$$

$$C_p^*(T) = \frac{h_i^j - h_i^{j-1}}{T_i^j - T_i^{j-1}} \tag{6}$$

where: C_p is the specific heat of the material, J/(kg K);
T is the temperature of each node, °C;
i is the current node;
j is the current time step;
ρ is the material density, kg/m^3;
Δx is the difference molecular layer thickness, m;
Δt is the time step, s;
k_w, k_e are the thermal conductivity between adjacent molecular layer materials, W/(m k);
c is spatial dispersion constant;
α is thermal diffusivity of materials.
h is the enthalpy of the substance, kJ/kg.

In CondFD algorithm, the data was automatically separated and discretized according to Eq. (4). It kept the default spatial discretization constant (C) of the algorithm unchanged and entered other values for calculation.

In this algorithm, it defines the relationship between the enthalpy value of PCM and temperature by defining Eqs. (5) and (6) (Qu et al., 2020; Xie et al., 2018a). The purpose of this is to establish the equivalent specific calorific value in each calculation. This model is an improved version of the original enthalpy method.

In this paper, meteorological environment of Shanghai (CHN_Shanghai. Shanghai.583620_SWERA) was selected as weather conditions, and the experimental model (a small confined space with double layer PCMs) and the reference model (the same small confined space without PCMs) were simulated based on EnergyPlus 9.0 version. The purpose of simulation is to investigate the temperature variations and energy consumption inside the building model. In the simulation of temperature of the model, the experimental model and the reference model did not set air conditioning, it compared the difference of indoor temperature between the experimental and the reference models. In the simulation of energy consumption in closed small space, the working period of air conditioning should be set. The working time of the air conditioner is from 7:00 to 24:00 every day, and the simulation span is year-round.

3. Experimental approach

3.1. Experimental materials

The comfortable indoor temperature of the building is 24–26 °C in the summer and 17–22 °C in the winter, the PCM with the melting point of 29 °C was selected for the external wall and the PCM with the melting point of 18 °C was selected for the internal wall. When the air conditioning is used, the temperature of inner wall is above 18 °C, the phase change material will undergo a phase change process with heat absorption. When the air conditioning is turned off, the temperature of the inner wall decreases, and the PCM will undergo another phase change to release the stored heat if the wall temperature is below the phase change point. In addition, EG was added to the PCM to improve the thermal performance of composite materials.

The paraffin wax with a melting point of 29 °C was put into a muffle furnace to be heated and melted, and then EG and paraffin wax were mixed with a ratio of 2:8 to prepare a composite PCM. In order to solve the problem of uneven contact between paraffin and EG, a multi-layer adsorption method was adopted (Guo et al., 2021; Liu et al., 2021), paraffin and EG were alternately distributed in the beaker. Compared with single-layer adsorption, multi-layer adsorption can make paraffin, EG contact more effectively, and achieve better adsorption effect. The paraffin wax with a melting point of 18 °C is liquid at room temperature. In order to avoid the leakage of the EG/paraffin composite PCM during the melting process, the paraffin was encapsulated in a small aluminium foil bag, as shown in Fig. 2a. The aluminium foil bags filled with PCM composites were evenly attached to the concrete slab. A copper plate was applied to fix the aluminium foil bags and provide uniformly heat flux from the electric heating film. In addition, the copper plate improved the curing and forming effect of the PCM in the horizontal (floor and roof) and vertical (south wall) aluminium foil bags. The size of each small aluminium foil bag is 10 cm $\times$10 cm, thereby it is necessary to attach 9 aluminium foil bags on the external and internal walls for the roof and south wall respectively. The floor was applied with a single layer of 9 aluminium foil bags. The thickness of aluminium bag with PCM is 10 mm.

3.2. Experimental apparatus

In order to measure the temperature change of PCMs in practice, a data acquisition instrument was employed to measure the specific temperature change process. The data acquisition object of the data acquisition board is the measuring temperature point, thereby T-type thermocouple was selected to measure the temperature of the measuring point. In order to ensure a more continuous and stable heat flow during the heating process of the electric heating film, a copper plate was added to the test surface to heat the PCM as shown in Fig. 2(b). In view of the similarity principle of each part of the same surface of the building model in the heat transfer process, the temperature measurement points in this paper were buried in the lower left quarter of the top surface. The T-type thermocouple was embedded in the PCM layer, and Fig. 2(c) is the schematic diagram of specific temperature measurement points. The test area is the lower left quarter of each wall, where 13 thermocouples are arranged. Fig. 2(d) presents the experimental flow chart. During the experiment, heating was performed by wrapping the model with an electric heating film, and the heat flow was kept as constant during the heating process.

In order to validate the numerical model, it carried out experiment and computational simulation in point 13 without adding PCMs, the results are plotted in Fig. 2(e). It found that the temperature has small numerical differences, and there was a significant transformation in the middle part, which was consistent with the previous test results. The value of average temperature difference is 0.5 °C, it indicates the numerical model has a high reliability.

4. Results and discussion

4.1. Simulation results of temperature and energy consumption in Shanghai

To understand the effect of PCMs, it compared simulation results of the central point temperature with or without PCM in the cubic model. Fig. 3(a) and (b) show the temperature conditions of the cubic model with and without PCMs of Shanghai in July and December. By comparing the temperature change curves of the two building models, it can be concluded that the use of PCMs can reduce the internal temperature of the model. When the PCM was made into a double-layer shaped phase change plate, the average temperature inside the model dropped by 1.5 °C. This

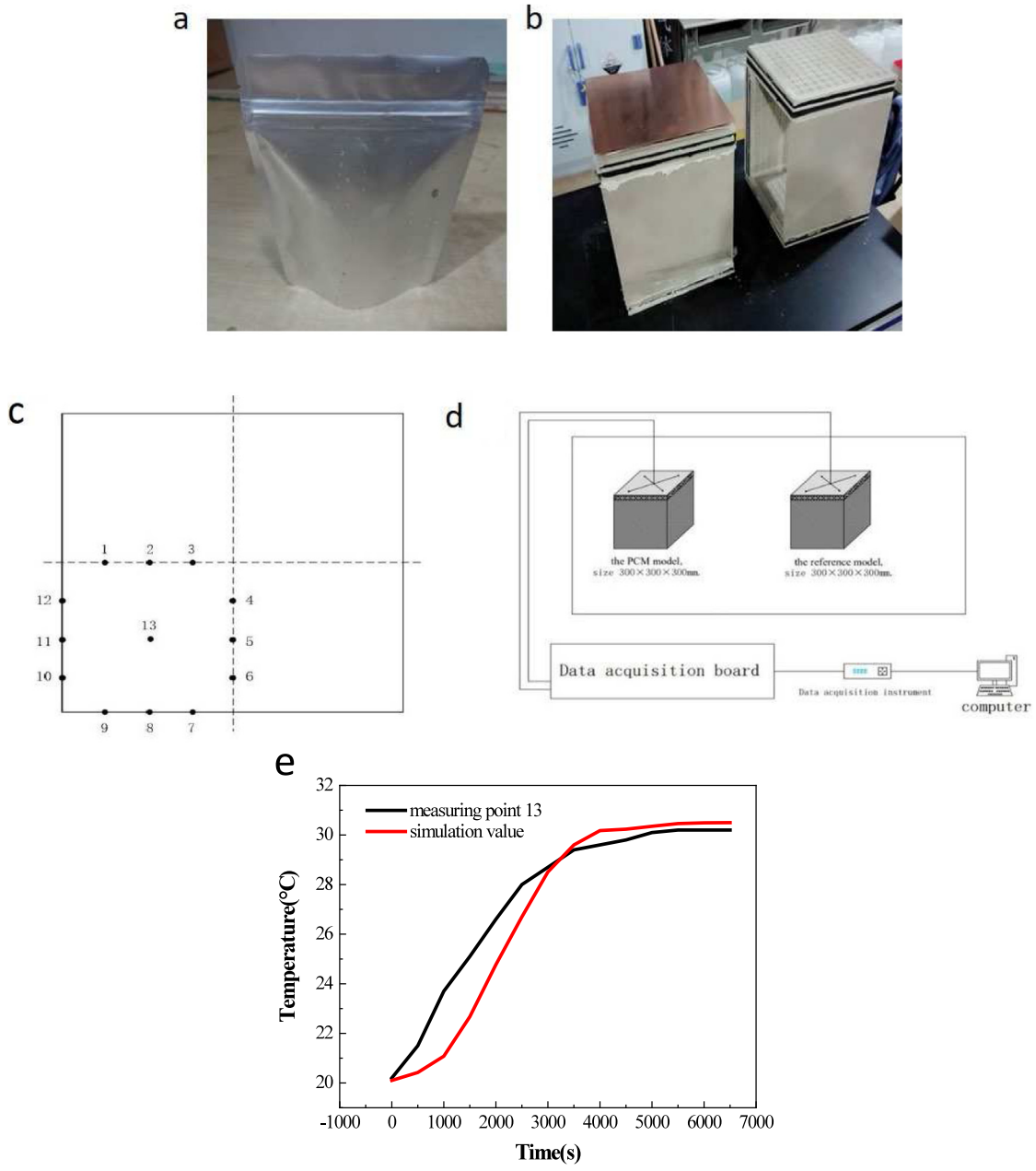

Fig. 2. (a) Aluminium foil bag containing PCM, (b) Experiment model. (c) Schematic diagram of temperature measurement points. (d) Experiment flow chart, (e) measured and simulated temperature of point 13 without PCM.

is attributed to the external PCM absorbed a lot of heat during the melting process. Meanwhile, the presence of the insulation board also prevented the introduction of external heat, reflecting a certain insulation effect. However, the effect of delaying peak temperature is not obvious. As shown in Fig. 3(c) and (d), the summer cooling load of the cubic models are also reduced. In July and August, when the average temperature was the highest, the cooling load of the model was reduced by 2000 J and 2500 J, respectively. In addition, in the winter, the internal PCM material provided thermal insulation, which also reduced the heating load of Shanghai in December by 15%.

Fig. 4(b) and (d) show that when there is no EG in the outer wall, the wall starts to enter the phase transition process at 2200 s and ends at 6400 s. When EG is added, the phase change process of the wall surface is from 2000 s to 5000 s. In contrast, the high thermal conductivity of EG allows the phase change process to start much earlier, reducing the phase change process by 40%.

Fig. 5(a) and (c) show that when the inner wall has no EG, the PCM starts to melt from 2200 s to 6400 s. In Fig. 5(b) and (d), the PCM with EG started to melt in 2000 s and ends in 5000 s. Meanwhile, the above figure shows the effect of EG on the melting process of PCM in the inner wall of model. When there is no EG, the liquid phase ratio increased to 1 from 2200 s to 6400 s. When EG is present, the liquid phase ratio increased to 1 from 2000 s to 5000 s. Therefore, the rate of change in the liquid phase liquid phase ratio is consistent with the time required for temperature changes with or without EG.

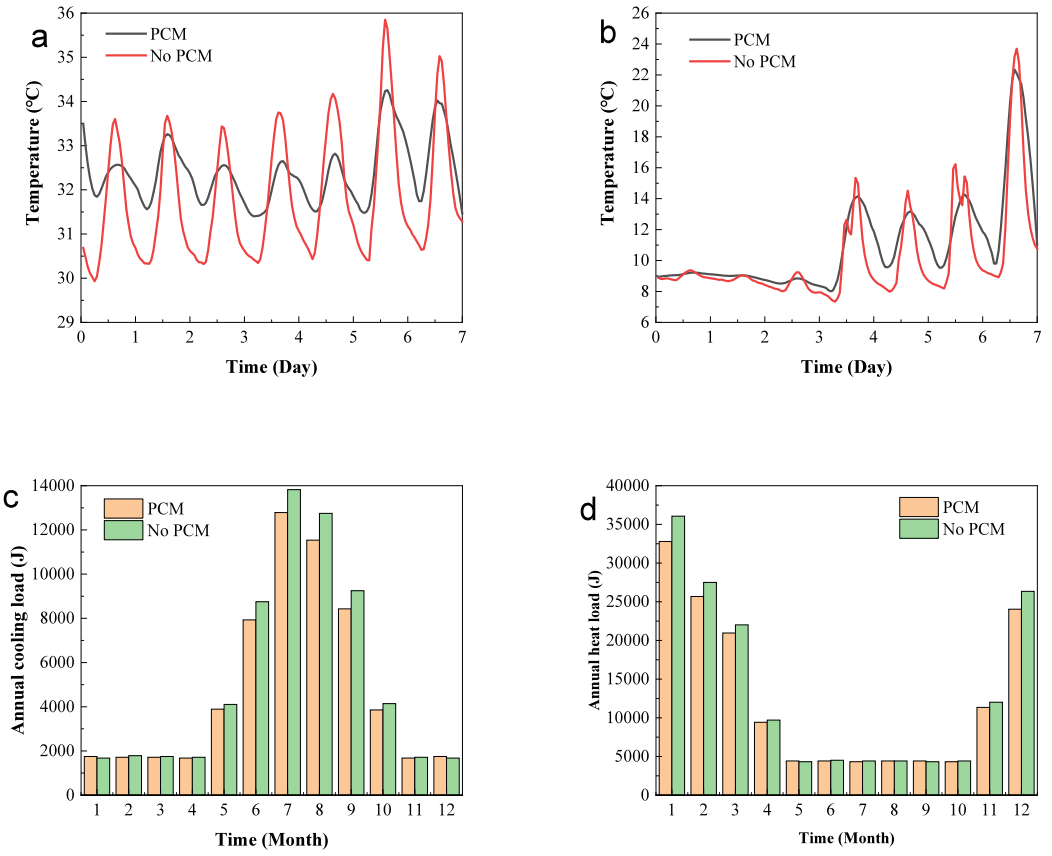

Fig. 3. Shanghai in (a) July and (b) December the first week with or without phase transition temperature change curve and annual (c) cooling and (d) heating load.

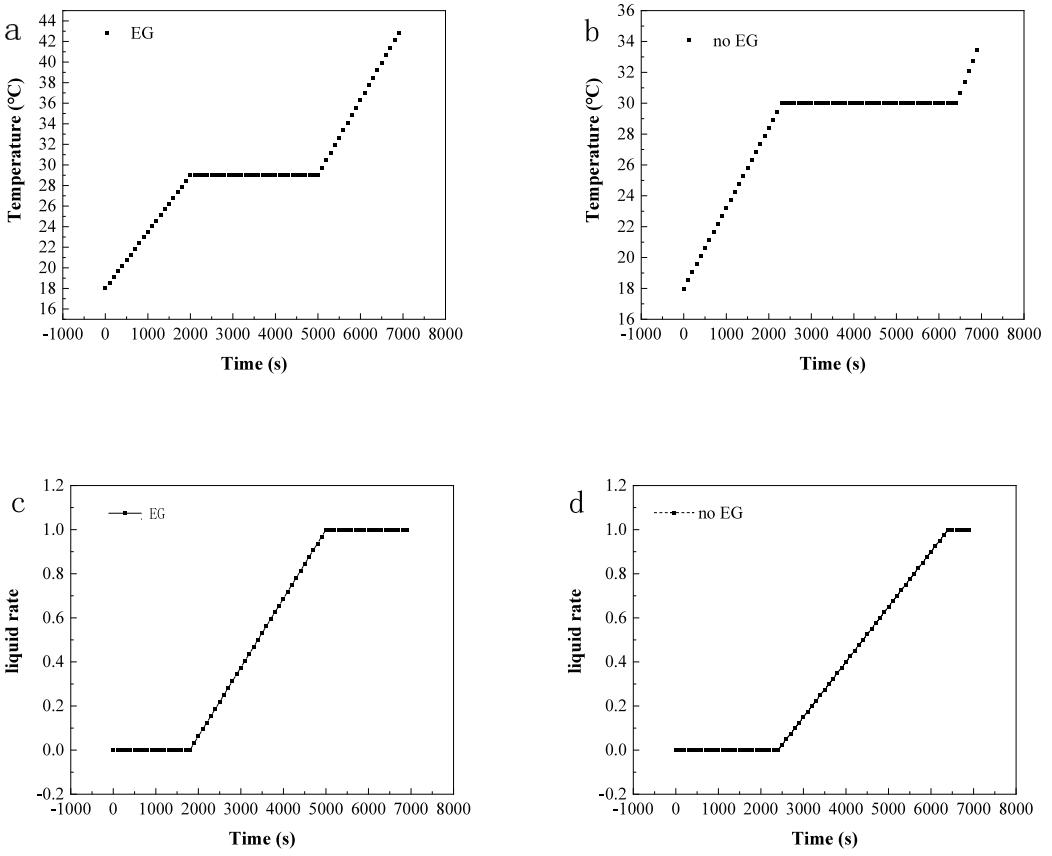

Fig. 4. Temperature change and liquid phase ratio of the outer paraffin (a) (c) with and (b) (d) without EG during the melting process.

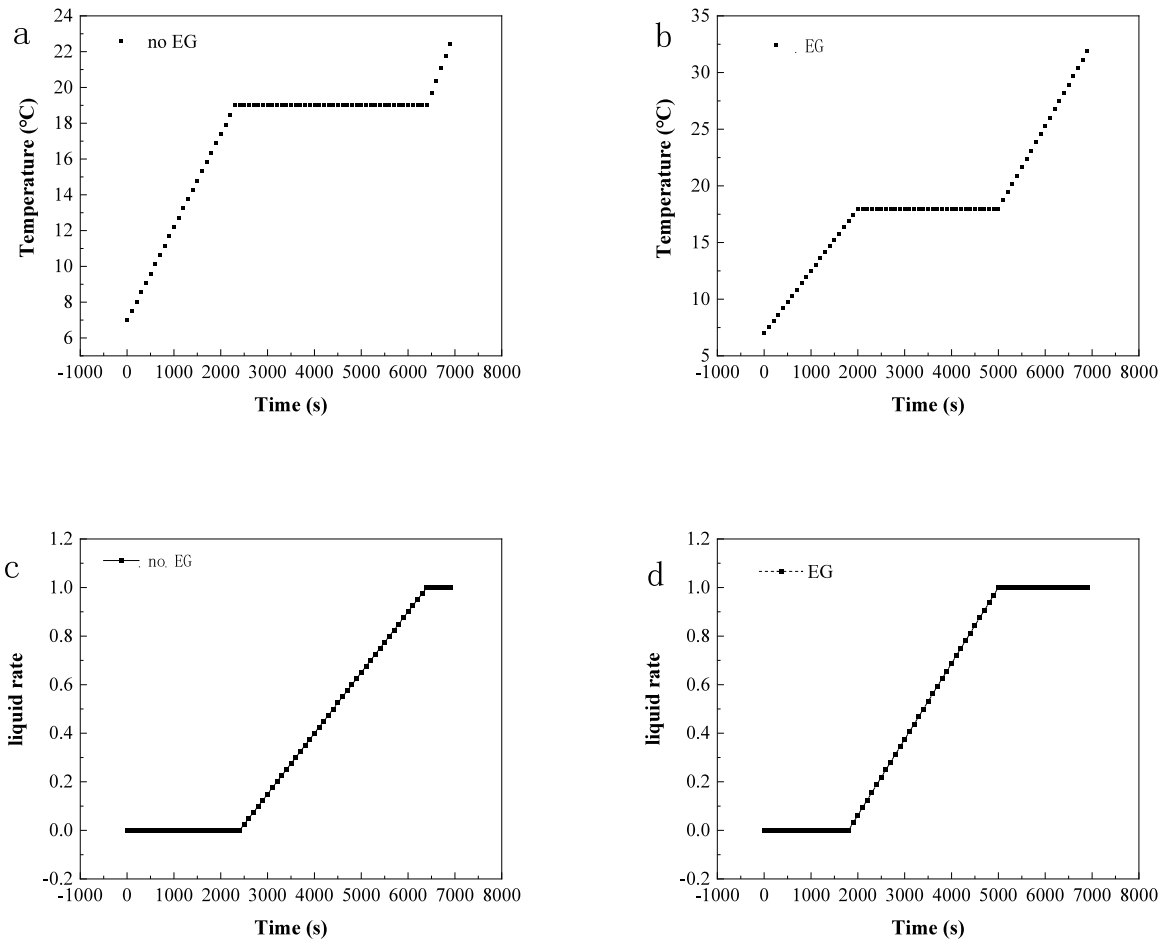

Fig. 5. Temperature change and liquid phase ratio of the inner paraffin (b) (d) with and (a) (c) without EG during the melting process.

4.2. Experimental temperature analysis

The DSC (differential scanning calorimetry) curves of the four paraffin are shown in Fig. 6. It can be seen from the figure that the addition of EG can advance the started melting point of paraffin and reduce the maximum heat flow rate of the mixtures. Fig. 7 is the change curve of thermal conductivity of four different melting paraffin added with EG. It can be seen that EG has obviously improved the thermal conductivity of paraffin.

Fig. 8(a) shows the temperature change curves of the measuring points 1, 2 and 3 in the outer wall during the melting process. It can be seen from the figure that the temperatures of the measuring points 1, 2 and 3 are basically the same in the initial state, all of which are solid at room temperature. Similarly, after the phase change process was completed, the PCMs were almost all in the liquid state and the temperatures of the measuring points 1, 2 and 3 are also basically the same. It can be seen from the figure that the point where the temperature difference is large during the phase change process due to the PCM coexists in the solid–liquid state. When the liquid component was increased, the thermal conductivity was stronger, and the temperature was correspondingly higher. Therefore, the heating conditions of these three measuring points are not necessarily the same, and there is a certain temperature deviation. However, the temperature range of the three is not much different, and the floating range does not exceed 2 °C. By comparing the average value of the measurement points 1, 2 and 3 with the simulated value as shown in Fig. 8(b), the average value is about 1 °C lower, and the temperature at the end of the phase change process is 1 °C higher than the simulated value. However, an error zone appears at the end of the phase change process. The experimental value is about 2 °C lower than the simulated value. This is mainly attributed to the PCM has a longer delay time in the simulated results. In the case of the experiment, due to the limitation of the experimental conditions, the building model could not be completely insulated, resulting in the measured temperature being lower than the simulated value. Fig. 8(c) shows the temperature changes of the outer wall points 4, 5 and 6 during the melting process. Compared with the above three measurement points, the melting process is similar. The difference is that the temperatures at points 4, 5 and 6 at the beginning of the phase change process are basically the same, and a temperature difference will occur during and at the end of the phase change process. This difference is also due to the different liquid phase ratios of the PCMs at different positions during the phase change process and the different heating conditions. Fig. 8(d) is the changes of average and simulated values of the three measurement points. The trends are still similar to the above figure, and as the building model cannot be completely insulated, the experimental values are lower than the simulated values.

Fig. 9(a) and (b) show the temperature changes at points 7, 8 and 9 during the melting process of the outer wall PCM. These three measuring points are basically consistent before and after the phase transition process. Before the start of the phase change

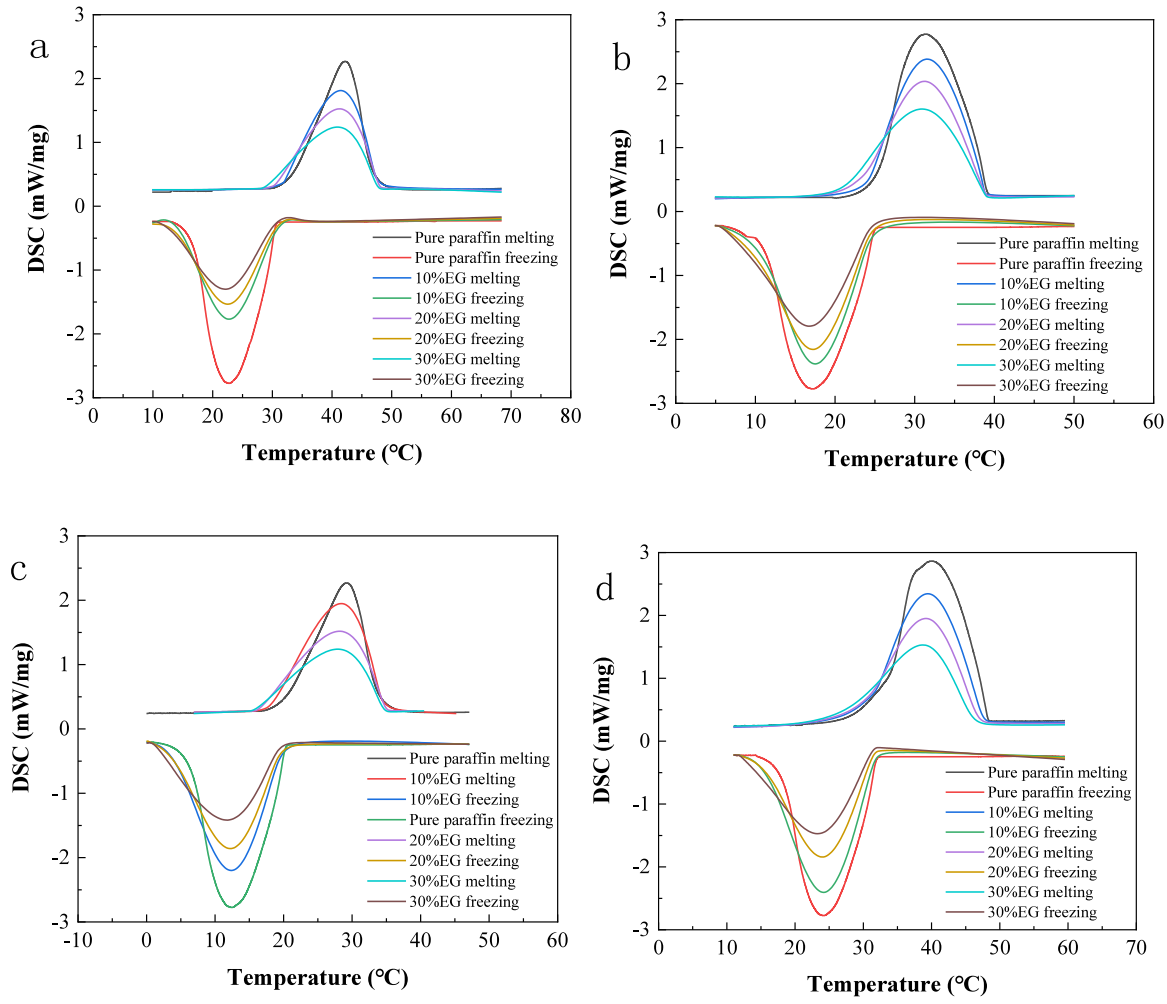

Fig. 6. DSC test curve of paraffin with melting point of (a) 31–33 °C, (b) 24–26 °C, (c) 18–20 °C, and (d) 29–31 °C.

process, the temperature difference of the three points does not exceed 0.5 °C. In the phase transition process, the heating process curves of the three points are almost the same. The temperature changes during the three phase transitions are slightly different, but the overall trend is the same. It is still found that the experimental value is lower than the simulated value at the end of the phase transition. Fig. 9(c) and (d) show the temperature changes at points 10, 11 and 12 during the melting process of the outer wall PCM. The trend is the same as the previous curve, and the temperatures at the three measurement points show a little difference during the phase transition period. The difference between the average and simulated values is the same as the above figure.

Fig. 10(a) and (b) show the temperature change curves of the measuring points 1, 2 and 3 in the inner wall during the melting process. The average value A is the average temperature of the measuring points 1, 2 and 3. It can be seen from the figure that in the measurement process, the data of the measurement points 1, 2 and 3 are slightly different, and the initial heating process is basically the same. At this time, when the paraffin/EG composite PCM was encapsulated, both were in a solid state, and the paraffin and EG are sufficiently mixed together. The selected measuring points 1, 2 and 3 are heated, and the temperature changes at these three positions are not much different. After the phase change process was completed, the paraffin wax was completely melted and almost entirely in the liquid state. The difference between the average curve of the three measurement points and the simulation curve is mainly due to the heat loss during the experiment. Fig. 10(c) and (d) show the temperature changes at points 4, 5 and 6 in the inner wall during the melting process. Compared with measuring points 1, 2 and 3, the melting process is roughly similar. The difference is that the temperature at the beginning of the phase change process at points 4, 5 and 6 is different, and the temperature curves are also inconsistent. This may be caused by the incomplete mixture of paraffin and EG at these three measurement points. Adsorption causes uneven mixing of materials at points 4, 5 and 6. As the thermal conductivity of paraffin and EG is extremely different, but the temperature difference between the three points does not exceed 0.5 °C, thereby it is still in an acceptable range.

Fig. 11(a) and (b) show the temperature changes at points 7, 8 and 9 in the inner wall during the melting process. Compared with measuring points 4, 5 and 6, the melting process is similar. The difference is that the temperature difference at the beginning of the phase change process at points 7, 8 and 9 is small and the temperature curves almost coincide. This might be due to the more uniform mixing of paraffin and EG at these three measurement points. In the phase transition process, paraffin wax melted by the heating process, and then it was gradually mixed with the EG. Fig. 11(c) and (d) show the temperature changes at the

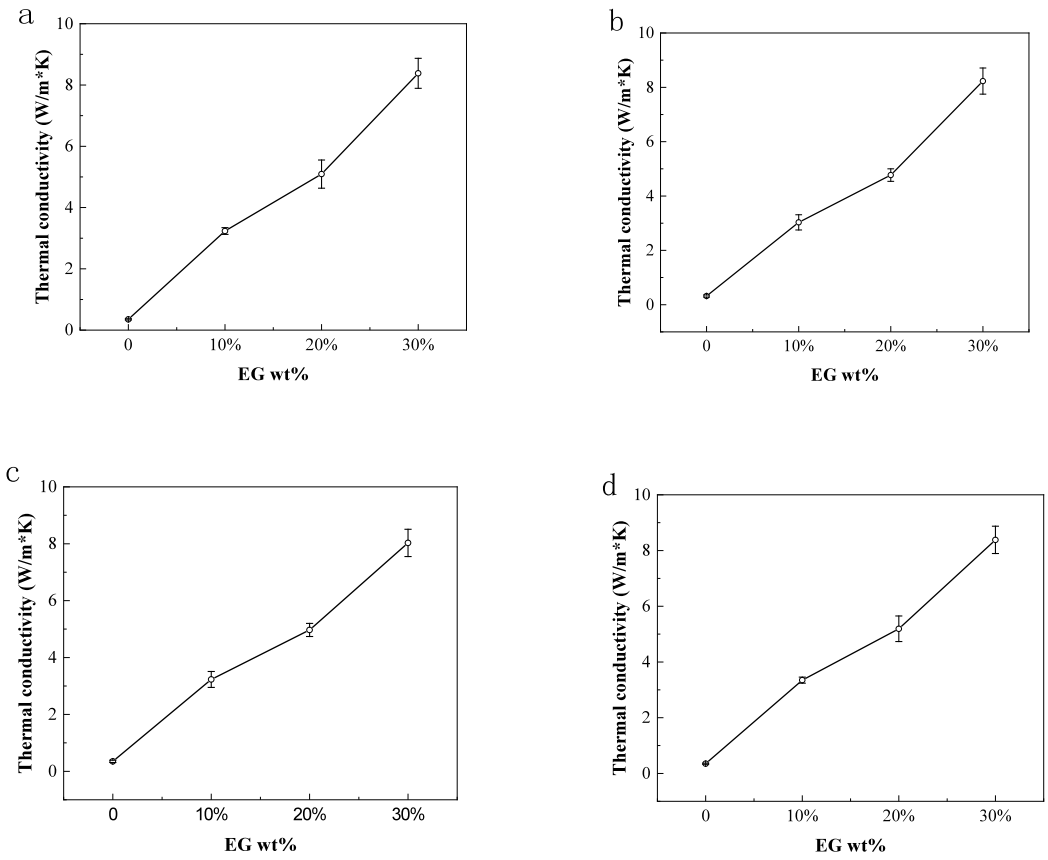

Fig. 7. The thermal conductivity of four paraffin with different melting points of (a) 18–20 °C, (b) 24–26 °C, (c) 29–31 °C, and (d) 31–33 °C with different proportions of EG.

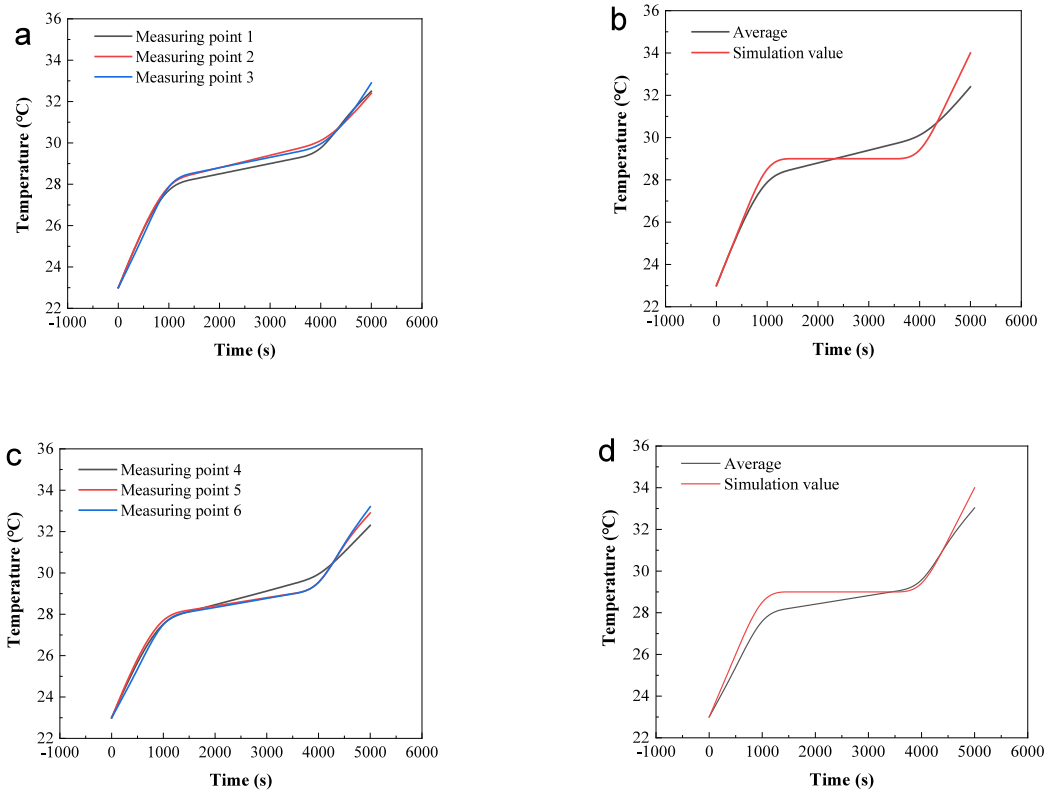

Fig. 8. (a) The melting process diagram of paraffin wax at measuring point 1, 2 and 3 in the outer wall. (b) The comparison between the average temperature at measuring points 1, 2 and 3 and the simulation results. (c) Diagram of paraffin melting process at measuring points 4, 5 and 6 in the outer wall, and (d) comparison of average temperature at measuring points 4, 5, 6 and simulation results.

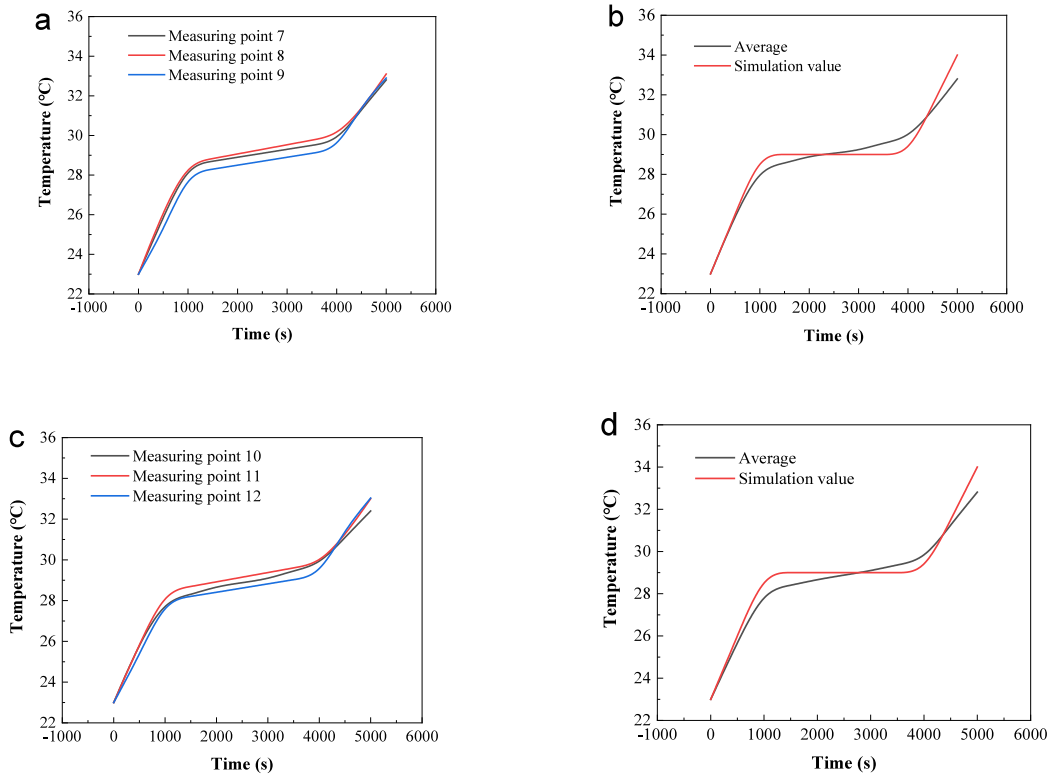

Fig. 9. (a) Diagram of paraffin melting process at measuring points 7, 8 and 9 in the outer wall, (b) comparison of average temperature at measuring points 7, 8, 9 and simulation results. (c) Diagram of paraffin melting process at measuring points 10, 11 and 12 in the outer wall, and (d) comparison of average temperature at measuring points 10, 11, 12 and simulation results.

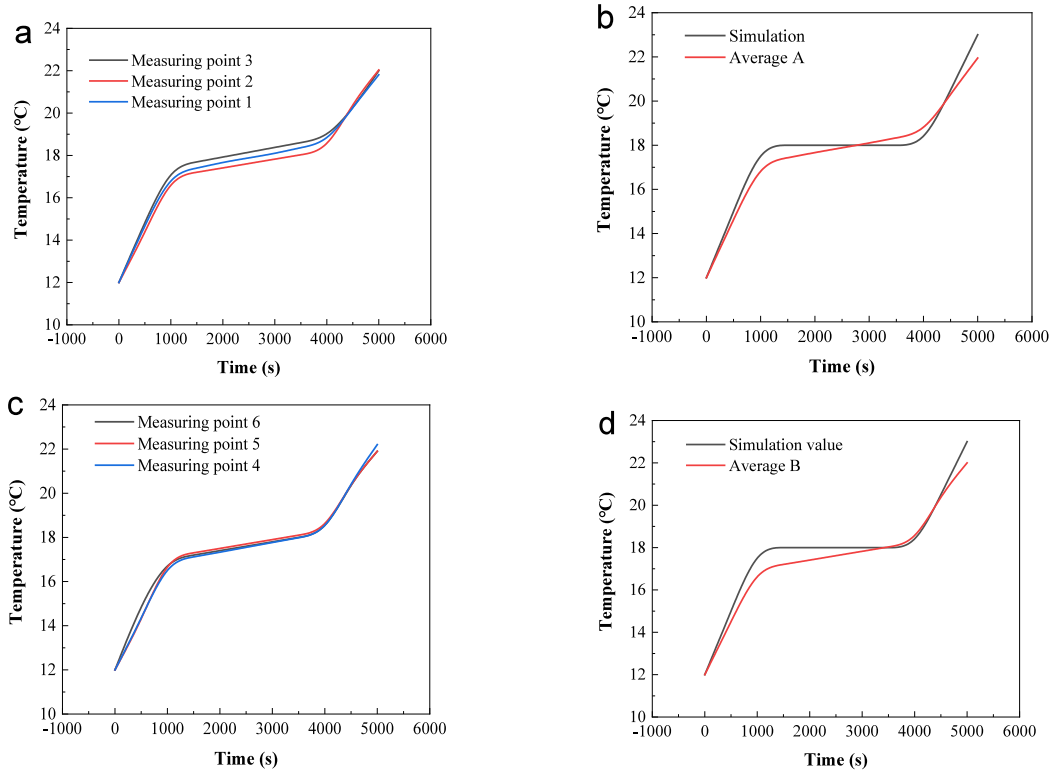

Fig. 10. (a) Diagram of paraffin melting process at measuring points 1, 2 and 3 in the inner wall, (b) comparison of average temperature at measuring points 1, 2, 3 and simulation results. (c) Diagram of paraffin melting process at measuring points 4, 5 and 6 in the inner wall, and (d) comparison of average temperature at measuring points 4, 5, 6 and simulation results.

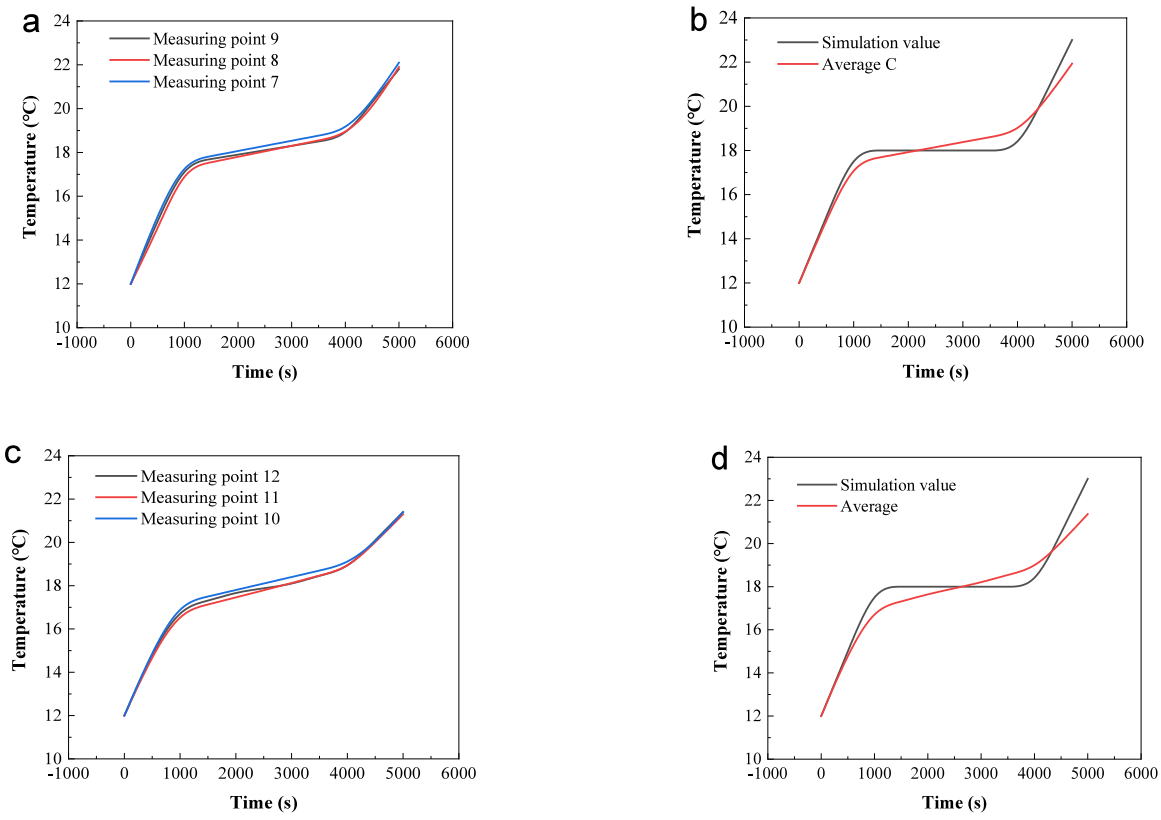

Fig. 11. (a) Diagram of paraffin melting process at measuring points 7, 8 and 9 in the inner wall, (b) comparison of average temperature at measuring points 7, 8, 9 and simulation results. (c) Diagram of paraffin melting process at measuring points 10, 11 and 12 in the inner wall, and (d) comparison of average temperature at measuring points 10, 11, 12 and simulation results.

measuring points 10, 11 and 12 during the melting process of the PCM in the inner wall. During the heating process before melting, the temperature of the three measurement points is almost the same, and the difference during the phase transition is relatively large. The temperature difference between the three can reach a maximum of 1 °C. A lower temperature indicates that more PCMs absorb the heat and melt in a liquid state during this time period. The simulated values present a constant phase change temperature in comparison with the experimental values during the phase change process.

Fig. 12(a) shows the temperature change of the measuring point 13 during the melting process of the PCM in the outer wall. Since the measuring point 13 is located in the middle of the temperature measurement area, its temperature change is more representative and convincing in theory. By comparing the temperature change of the measuring point 13 with the simulated value, it is not difficult to find that the temperature change trend before and during the phase change process is consistent. Fig. 12(b) shows the temperature change of the measurement point 13 during the melting process of the PCM in the inner wall. By comparing the temperature change at the measurement point 13 with the simulated value, it is can be found that the simulated value has risen from 12 °C to 18 °C before the start of the phase transition process, and the experimental value is consistent with the theoretical temperature change trend during the phase transition process. Fig. 12(c) shows the comparison between the average temperature of the measuring point 13 and the simulated value in the outer wall. It can be concluded that the PCM started to enter the phase change process at approximately 1000 s and completed at approximately 4000 s. In the initial stage, the simulated value is basically consistent with the experimental value. After entering the phase change process, the temperature changes of the PCM increased slowly. At this time, the PCM melted and absorbed the heat, but the overall heat conduction was still in progress. At the end of the phase transition process, the experimental value was 2 °C lower than the simulated value, it is mainly caused by the model cannot be completely insulated during the experimental process. Fig. 12(d) shows the comparison between the average temperature of the measuring point 13 and the simulated value in the inner wall. The melting mechanism of the internal and external PCMs are similar. The PCM started to enter the phase change phase in approximately 1000 s, and the phase change process was completed in approximately 4000 s. At the beginning of the heating process, the simulated value is basically consistent with the experimental value. After entering the phase change process, the temperature changes of the PCM slowly increased. As the heat conduction phenomenon in the PCM continued to occur, the composition of liquid paraffin and the temperature increased gradually. Compared with the image trend in the first stage, the rate of temperature increased was slower. At the end of the phase change process, the experimental value was about 1.8 °C lower than the simulated value. This is mainly due to the heat loss during the experimental process. In the context of phase change materials inexistence, it compared the changes of measured and simulated temperatures of the model in 6500 s.

5. Conclusion

In this paper, a double layer phase change composite wall was applied to the roof, south wall of the cubic building model. The inner and outer layers of composite walls used PCMs with different melting points to regulate the indoor temperature in the summer and winter, respectively. The following conclusions can be drawn based on the experimental and numerical analysis:

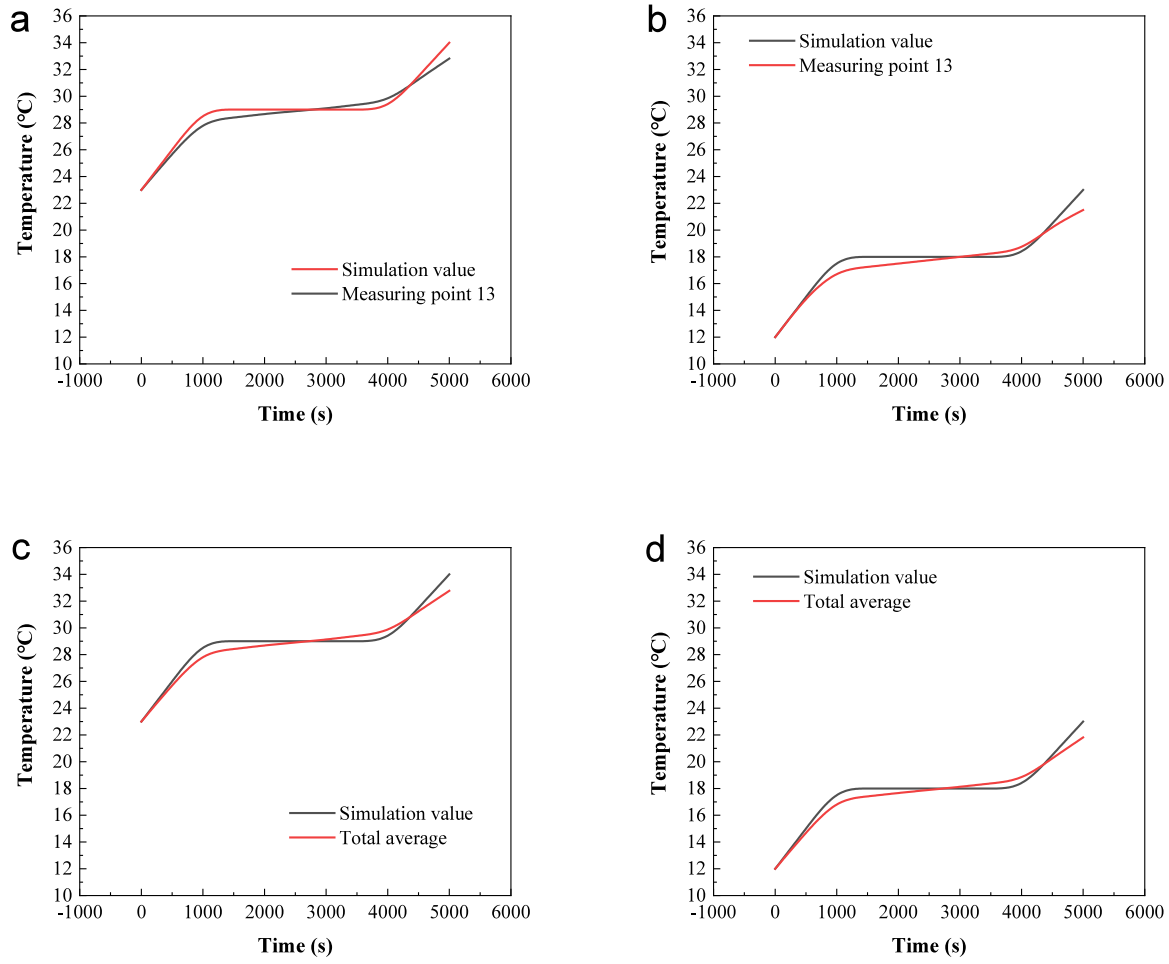

Fig. 12. The temperature changes of the outer (a) and the inner (b) walls for measuring point 13 and the comparison of the average and simulated values of the outer (c) and inner (d) walls measuring point temperatures.

(1) EG can shorten the time required for the phase change process. When the external temperature and the melting point of the PCM are not much different, the PCM melts slowly due to poor thermal conductivity. It cannot absorb the heat and prevent heat being transferred to the room, thereby it is necessary to improve the thermal conductivity of PCM composites.

(2) Double layer phase change wall significantly reduced energy consumption in the Shanghai area and maintained the internal temperature for a longer time. The cooling load of the model in the summer was reduced more than 2000 J. In the winter, it reduced the heating load by 15%. The average temperature in the model was dropped by 1.5 °C.

(3) In the initial stage, the simulated values were consistent with the experimental values. At the end of the phase change process, the phase change process in the simulation was longer than the experiment due to the heat loss in the experiment, thereby the actual temperature was lower than the simulated value. The three measuring points on the same line have a temperature deviation. However, the variation is small, and the maximum temperature variation does not exceed 1 °C.

In summary, for rural areas in northern China, the application of such phase change walls as thermal insulation materials in newly built residences can improve the indoor thermal comfort and reduce the building energy consumption. Therefore, the double layer phase change composite wall proposed in this paper has great application prospects in energy saving for small and medium-sized independent buildings in the middle and high latitudes area.

CRediT authorship contribution statement

Hanxue Yang: Validation, Formal analysis, Data curation, Writing – review & editing, Visualization. **Guanhua Zhang:** Supervision, Project administration, Funding acquisition. **Binlin Dou:** Supervision, Funding acquisition. **Xiaoyu Yan:** Supervision, Project administration. **Zhiqiang Liu:** Investigation, Resources. **Wenchao Qi:** Methodology, Conceptualization, Software, Writing – original draft.

Declaration of competing interest

The authors declare that they have no known competing financial interests or personal relationships that could have appeared to influence the work reported in this paper.

Acknowledgements

This work was supported by the National Natural Science Foundation of China (No. 51976126), Youth Eastern Scholar Program of Shanghai Municipal Education Commission, Shanghai Municipal Science and Technology Committee of Shanghai outstanding academic leaders plan (No. 21XD1402400)

References

Bao, X., Yang, H., Xu, X., Xu, T., Cui, H., Tang, W., et al., 2020. Development of a stable inorganic phase change material for thermal energy storage in buildings. Sol. Energy Mater. Sol. Cells 208.

Behi, M., Mirmohammadi, SA., Ghanbarpour, M., Behi, H., Palm, B., 2018. Evaluation of a novel solar driven sorption cooling/heating system integrated with PCM storage compartment. Energy 164, 449–464.

Cellura, M., Guarino, F., Longo, S., Tumminia, G., 2018. Climate change and the building sector: Modelling and energy implications to an office building in southern europe. Energy Sustain. Dev. 45, 46–65.

Chen, Y., Hong, T., Piette, MA., 2017. Automatic generation and simulation of urban building energy models based on city datasets for city-scale building retrofit analysis. Appl. Energy 205, 323–335.

Chen, F., Huang, R., Wang, C., Yu, X., Liu, H., Wu, Q., et al., 2020. Air and PCM cooling for battery thermal management considering battery cycle life. Appl. Therm. Eng. 173, 115154.

Du, K., Calautit, J., Wang, Z., Wu, Y., Liu, H., 2018. A review of the applications of phase change materials in cooling, heating and power generation in different temperature ranges. Appl. Energy 220, 242–273.

Dutkowski, K., Fiuk, JJ., 2018. Experimental investigation of the effects of mass fraction and temperature on the viscosity of microencapsulated PCM slurry. Int. J. Heat Mass Transf. 126, 390–399.

Fredi, G., Dorigato, A., Unterberger, S., Artuso, N., Pegoretti, A., 2019. Discontinuous carbon fiber/polyamide composites with microencapsulated paraffin for thermal energy storage. J. Appl. Polym. Sci. 136, 47408.

Fu, L., Wang, Q., Ye, R., Fang, X., Zhang, Z., 2017. A calcium chloride hexahydrate/expanded perlite composite with good heat storage and insulation properties for building energy conservation. Renew. Energy 114, 733–743.

Ghadbeigi, L., Day, B., Lundgren, K., Sparks, TD., 2018. Cold temperature performance of phase change material based battery thermal management systems. Energy Rep. 4, 303–307.

Gholamibozanjani, G., Farid, M., 2020. Peak load shifting using a price-based control in PCM-enhanced buildings. Sol. Energy 211, 661–673.

Gil, A., Medrano, M., Martorell, I., Lázaro, A., Dolado, P., Zalba, B., et al., 2010. State of the art on high temperature thermal energy storage for power generation, part 1—Concepts, materials and modellization. Renew. Sustain. Energy Rev. 14, 31–55.

Guo, H., ELSihy, ES., Liao, Z., Du, X., 2021. A comparative study on the performance of single and multi-layer encapsulated phase change material packed-bed thermocline tanks. Energies 14, 2175.

Jin, X., Zhang, X., 2011. Thermal analysis of a double layer phase change material floor. Appl. Therm. Eng. 31, 1576–1581.

Li, Y., Yan, H., Wang, Q., Wang, H., Huang, Y., 2017. Structure and thermal properties of decanoic acid/expanded graphite composite phase change materials. J. Therm. Anal. Calorim. 128, 1313–1326.

Lin, Y., Alva, G., Fang, G., 2018. Review on thermal performances and applications of thermal energy storage systems with inorganic phase change materials. Energy 165, 685–708.

Liu, L., Chen, J., Qu, Y., Xu, T., Wu, H., Huang, G., et al., 2019a. A foamed cement blocks with paraffin/expanded graphite composite phase change solar thermal absorption material. Sol. Energy Mater. Sol. Cells 200.

Liu, L., Li, J., Deng, Y., Yang, Z., Huang, K., Zhao, S., 2021. Optimal design of multilayer structure composite containing inorganic hydrated salt phase change materials and cement: Lab-scale tests for buildings. Constr. Build. Mater. 275, 122125.

Liu, J., Liu, Y., Yang, L., Liu, T., Zhang, C., Dong, H., 2020. Climatic and seasonal suitability of phase change materials coupled with night ventilation for office buildings in western China. Renew. Energy 147, 356–373.

Liu, Z., Zhang, S., Hu, D., Zhang, Y., Lv, H., Liu, C., et al., 2019b. Paraffin/red mud phase change energy storage composite incorporated gypsum-based and cement-based materials: Microstructures, thermal and mechanical properties. J. Hazard. Mater. 364, 608–620.

Lu, W., Liu, G., Xiong, Z., Wu, Z., Zhang, G., 2020. An experimental investigation of composite phase change materials of ternary nitrate and expanded graphite for medium-temperature thermal energy storage. Sol. Energy 195, 573–580.

Maleki, M., Karimian, H., Shokouhimehr, M., Ahmadi, R., Valanezhad, A., Beitollahi, A., 2019. Development of graphitic domains in carbon foams for high efficient electro/photo-to-thermal energy conversion phase change composites. Chem. Eng. J. 362, 469–481.

Mankel, C., Caggiano, A., Koenders, E., 2019. Thermal energy storage characterization of cementitious composites made with recycled brick aggregates containing PCM. Energy Build. 202.

Markarian, E., Fazelpour, F., 2019. Multi-objective optimization of energy performance of a building considering different configurations and types of PCM. Sol. Energy 191, 481–496.

Qu, Y., Wang, S., Zhou, D., Tian, Y., 2020. Experimental study on thermal conductivity of paraffin-based shape-stabilized phase change material with hybrid carbon nano-additives. Renew. Energy 146, 2637–2645.

Roman, KK., O'Brien, T., Alvey, JB., Woo, O., 2016. Simulating the effects of cool roof and PCM (phase change materials) based roof to mitigate UHI (urban heat island) in prominent US cities. Energy 96, 103–117.

Saxena, R., Rakshit, D., Kaushik, S., 2020. Experimental assessment of phase change material (PCM) embedded bricks for passive conditioning in buildings. Renew. Energy 149, 587–599.

Skaalum, J., Groulx, D., 2020. Heat transfer comparison between branching and non -branching fins in a latent heat energy storage system. Int. J. Therm. Sci. 152.

Wang, C., Deng, S., Niu, J., Long, E., 2019. A numerical study on optimizing the designs of applying PCMs to a disaster-relief prefabricated temporary-house (PTH) to improve its summer daytime indoor thermal environment. Energy 181, 239–249.

Wang, H., Lu, W., Wu, Z., Zhang, G., 2020. Parametric analysis of applying PCM wallboards for energy saving in high-rise lightweight buildings in shanghai. Renew. Energy 145, 52–64.

Xie, J., Wang, W., Liu, J., Pan, S., 2018a. Thermal performance analysis of PCM wallboards for building application based on numerical simulation. Sol. Energy 162, 533–540.

Xie, J., Wang, W., Sang, P., Liu, J., 2018b. Experimental and numerical study of thermal performance of the PCM wall with solar radiation. Constr. Build. Mater. 177, 443–456.

Yang, YK., Kim, MY., Chung, MH., Park, JC., 2019. Pcm cool roof systems for mitigating urban heat island - an experimental and numerical analysis. Energy Build. 205.

Yun, BY., Park, JH., Yang, S., Wi, S., Kim, S., 2020. Integrated analysis of the energy and economic efficiency of PCM as an indoor decoration element: Application to an apartment building. Sol. Energy 196, 437–447.

Zhang, G., Cui, G., Dou, B., Wang, Z., Goula, MA., 2018. An experimental investigation of forced convection heat transfer with novel microencapsulated phase change material slurries in a circular tube under constant heat flux. Energy Convers. Manag. 171, 699–709.

Zhang, G., Yu, Z., Cui, G., Dou, B., Lu, W., Yan, X., 2020. Fabrication of a novel nano phase change material emulsion with low supercooling and enhanced thermal conductivity. Renew. Energy 151, 542–550.

Zhu, N., Hu, N., Hu, P., Lei, F., Li, S., 2019a. Experiment study on thermal performance of building integrated with double layers shape-stabilized phase change material wallboard. Energy 167, 1164–1180.

Zhu, N., Li, S., Hu, P., Lei, F., Deng, R., 2019b. Numerical investigations on performance of phase change material trombe wall in building. Energy 187, 116057.

Zhu, N., Liu, F., Liu, P., Hu, P., Wu, M., 2016. Energy saving potential of a novel phase change material wallboard in typical climate regions of China. Energy Build. 128, 360–369.

Ziasistani, N., Fazelpour, F., 2019. Comparative study of DSF, PV-DSF and PV-DSF/PCM building energy performance considering multiple parameters. Sol. Energy 187, 115–128.